International Journal of Numerical Methods for Heat & Fluid Flow

Numerical investigation of double-diffusive mixed convection in horizontal annulus partially filled with a porous medium

Mourad Moderres, Said Abboudi, Malika Ihdene, Sofiane Aberkane, Abderahmane Ghezal,

Numerical investigation of double-diffusive mixed convection in horizontal annulus partially filled with a porous medium

Mourad Moderres
Laboratoire de Mécanique des Fluides Théorique et Appliqué, Université des Sciences et de la Technoligie Houari Boumediene, Bab Ezzouar, Algiers, Algeria

Said Abboudi
IRTES-M3M, Université De Technologie De Belfort-Montbéliard, Belfort Cedex, France

Malika Ihdene
Université de Yahia Fares, Médéa, Algeria

Sofiane Aberkane
Université de M'hamed Bougara, Boumerdés, Algeria, and

Abderahmane Ghezal
Laboratoire de Mécanique des Fluides Théorique et Appliqué, Université des Sciences et de la Technoligie Houari Boumediene, Bab Ezzouar, Algiers, Algeria

Received 16 October 2015
Revised 1 March 2016
Accepted 3 March 2016

Abstract

Purpose – Double-diffusive convection within a tri-dimensional in a horizontal annulus partially filled with a fluid-saturated porous medium is numerically investigated. The aim of this work is to understand the effects of a source of heat and solute on the fluid flow and heat and mass transfer rates.

Design/methodology/approach – In the formulation of the problem, the Darcy–Brinkman–Forchheimer model is adopted to the fluid flow in the porous annulus. The laminar flow regime is considered under steady state conditions. Moreover, the transport equation for continuity, momentum, energy and mass transfer are solved using the Patankar–Spalding technique.

Findings – Through this investigation, the predicted results for both average Nusselt and Sherwood numbers were correlated in terms of Lewis number, thermal Grashof number and buoyancy ration. A comparison was made with the published results and a good agreement was found.

Originality/value – The paper's results are validated by favorable comparisons with previously published results. The results of the problem are presented in graphical forms and discussed. This paper aims to study the behavior of the flow structure and heat transfer and mass for different parameters.

Keywords Heat and mass transfer, Double-diffusive convection, Porous annulus, Radius ratio, Three-dimensional

Paper type Research paper

This research was supported by the Ministry of Higher Education and Scientific Research of Algeria through collaboration between the laboratory LMFTA of USTHB in Algeria and IRTES M3M of UTBM Belfort France.

International Journal of Numerical Methods for Heat & Fluid Flow
Vol. 27 No. 4, 2017
pp. 773-794

0961-5539
DOI 10.1108/HFF-10-2015-0434

Nomenclature

A = aspect ratio
C' = concentration, [$kg \cdot m^{-3}$]
C = dimensionless concentration, (=$(C' - C'_0)/(C'_i - C'_0)$)
C_F = Forchheimer Coefficient
D = mass diffusivity, [$m^2 s^{-1}$]
d = annulus gap width, (= $r_0 - r_i$)
e = thickness of the porous layer
g = gravitational acceleration, [$m.s^{-2}$]
Gr_S = solutal Grashof number based on the gap width, (=$g\beta_S(C_1 - C_0)d^3/\gamma^2$)
Gr_T = thermal Grashof number based on the gap width, (=$g\beta_T(T_1 - T_0)d^3/\gamma^2$)
k = permeability of the porous medium, m^2
Le = Lewis number, (=S_c/P_r)
N = Buoyancy ratio number, (=Gr_S/Gr_T)
Nu = local Nusselt number, (=$\ln(R_i/R_o)(R\partial\theta/\partial R)R_o$)
Nu_φ = average Nusselt number, (=$1/2\pi\int_0^{2\pi} Nu\, d\varphi$)
p = pressure, [$N.m^{-2}$]
P = dimensionless pressure
Pr = Prandtl number, (= γ/α)
r = radial coordinate, [m]
r_i, r_0 = inner and outer radii respectively, [m]
R = dimensionless radial coordinate, $R=r/d$
R_i, R_0 = dimensionless Inner and outer radii, respectively
Ra_S = solutal Reyleigh number based on the gap width, (=Gr_S.Pr)
Ra_T = thermal Reyleigh number based on the gap width, (=Gr_T.Pr)
Re = rotational Reynolds, (=$r_o \omega e/\gamma$)
Sc = Schmidt number, (= γ/D)
Sh = local Sherwood number, (=$\ln(R_i/R_o)(R\,\partial C/\partial R)R_o$)
Sh_φ = average Sherwood number, (=$1/2\pi\int_0^{2\pi} Sh\, d\varphi$)
T = local temperature, [K]
T_i, T_0 = temperature at inner and outer radii respectively, [K]
ΔT = temperature difference, (=T0 − Ti), [K]
(r, z, ϕ) = dimensional radial, axial and angular coordinates
(R, Z, φ) = dimensionless radial, axial and angular coordinates
(v_r, v_z, v_φ) = dimensional velocity components in (r, z, φ) directions, [$m.s^{-1}$]
(V_r, V_z, V_φ) = dimensionless velocity components in (r, z, φ) directions
R_μ = viscosity ratio, μ_{eff}/μ
R_λ = ratio of thermal conductivity, λ_{eff}/λ
R_D = ratio of solutal diffusivity, D_{eff}/D

Greek letters

λ = thermal conductivity, [$Wm^{-1}K^{-1}$]
α = thermal diffusivity, [$m^2 s^{-1}$]
β_S = solutal expansion coefficient, [$m^3 kg^{-1}$]
β_T = thermal expansion coefficient, [$m\,K^{-1}$]
ε = porosity
θ = dimensionless temperature, (= $(T - T_0)/(T_i - T_0)$)
ρ = density, [$Kg.m^{-3}$]
Ω = dimensionless velocity, s^{-1}

v = kinematic viscosity, $[m^2 s^{-1}]$
η = radius ratio
e_{ff} = effective
ψ = stream function
ω = dimensionless angular velocity, $\Omega(r_0 - r_i)/\Omega r_0$

Subscripts
i = inner cylinder
o = outer cylinder

1. Introduction

The heat and mass transfer in porous media have been of great increasing interest for several decades. Double-diffusive convection is referred to as the problem, where the fluid flow is induced by the simultaneous presence of two diffusive parameters: temperature and concentration. A substantial amount of research has been reported on double-diffusive convection in confined spaces because of its many engineering and technology applications. They include oil recovery techniques (steam flooding processes) in biomechanical problems (blood flow in the pulmonary alveolar sheet) and the technologies involved in the chemical vapor deposition processes for the semiconductor device fabrications. To improve the heat and mass transfer, researchers have developed a variety of effective strengthening heat transfer technologies, such as changing the surface structure to increase heat exchange area; using additives to change wall physical properties; inserting circular tube to change fluid flow characteristics; and so on. Porous substrate, as an efficient tool, is also used widely to enhance heat transfer in many engineering applications because of its high thermal conductivity and correlational studies are carried out in recent years.

Many authors as Vadasz (2008), Nield and Bejan (2006), Vafai (2005) have presented comprehensive literature review in this topic. They analyzed heat and fluid flow in porous domains in cylindrical and rectangular cavities. Most of the earlier works on the double diffusive convection are concerned with the onset of motion in a horizontal porous layer subject to vertical temperature and concentration gradients (Rudraiah *et al.*, 1982). Trevisan and Bejan (1986) were the first to examine some of the fundamental flow of characteristics of double-diffusive convection within a rectangular porous cavity subject to uniform fluxes of heat and mass from the side walls. Laminar natural convection in vertical porous annulus has widely been numerically and experimentally investigated in the literature. Havstad and Burns (1982) presented numerical results for the heat transfer with moderate cylinder spacing and for high temperature differences in a vertical annulus filled with a porous medium and presented correlations for the heat transfer in the annulus configuration. The phenomenon has been studied considering different boundary conditions, such as imposed temperature (Prasad and Kulacki, 1985; Rong *et al.*, 2010), as well as constant heat flux, at the wall (Prasad, 1986; Jha, 2005) for a wide range of Rayleigh numbers, aspect ratios and radius ratios. Char and Lee (1998) studied the effects of the radius ratio, aspect ratio, Forchheimer inertia parameter and Darcy number parameter to examine the natural convection of cold water in a vertical porous annulus using a finite difference method and the modified strongly implicit procedure and found that both the Forchheimer inertial parameter and the Darcy number have the same influence on the heat transfer characteristics; it is also found that the mean Nusselt number decreases as the Forchheimer inertia parameter or the Darcy number increases. From the analysis of the open literature,

fully explicit solutions, based on the finite element method, do not seem to be available for the problem under investigation.

Regarding natural convective flow in vertical porous annuli with internal heat generation, the analysis of the available literature shows that this topic has not been thoroughly investigated (Reddy and Narasimhan, 2010; Rao and Wang, 1991; Prasad and Chui, 1989). Documents on free convection in horizontal annuli, completely (Kumari and Nath, 2008; Roschina *et al.*, 2005; Aboubi *et al.*, 1998; Barbosa Mota and Saatdjian, 1995, 1997) or partially (Khanafer *et al.*, 2008; Reddy and Narasimham, 2008; Aldoss *et al.*, 2004) filled with a porous medium, are available, whereas the geometry of vertical partly porous annulus has been considered only with thermo-solutal convection flow (Benzeghiba *et al.*, 2003). Padilla and Silveira-Neto (2008) has used the large-eddy simulations method for identify the transition to turbulence in a horizontal annular cavity for vigorous natural convection. The onset of the transition to turbulence, the turbulence regime and the dynamic characteristics of the thermal plume transition were pointed out. The instantaneous and time average velocity and temperature fields were analyzed. The influence of both transitional and turbulent flows on the local and the mean Nusselt numbers were also investigated.

Forced convection, where the annular space is partially or completely filled with a fluid saturated porous medium, has been significantly analyzed (Mohamad, 2003; Pavel and Mohamad, 2004; Yang and Hwang, 2009). Mohamad (2003) investigated heat transfer enhancement for a flow in a pipe fully or partially filled with porous medium. Forced laminar flow was assumed, and the effects of porous layer thickness on the rate of heat transfer and pressure drop have been presented. The Darcy number was varied in the range of 10^{-6} to 10. The results show that the plug flow assumption is not valid for $\mathrm{Da} > 10^{-4}$, where the permeability of the medium is high. Inertia term has significant effect on the Nusselt number (Pavel and Mohamad, 2004). The effects of porosity, porous material diameter and thermal conductivity, as well as Reynolds number on the heat transfer rate and pressure drop, were studied experimentally and numerically. The pipe is subjected to a constant and uniform heat flux. The results obtained show that higher heat transfer rates can be achieved using porous inserts whose diameters approach the diameter of the pipe. Yang and Hwang (2009) investigated numerically the fluid flow behavior and heat transfer enhancements in a pipe fully or partially filled with porous medium inserted at the core of the conduit. The numerical results reveal that heat transfer can be enhanced by using high thermal conductivity porous inserts. Moreover, the turbulent flow in the conduit without porous medium can dissipate the heat from the heating wall because of the strong forced convectional effect, and the local distributions of the Nusselt number along the flow direction increase with the increase of the Reynolds number and the thickness of the porous layer but increase with the decreasing of the Darcy number. Alkam and Al-Nimr (1998), presented the transient forced convection in the developing region of a cylindrical channel partially filled with a porous substrate. The flow within the porous domain is modeled by the Brinkman–Forchheimer-extended Darcy model. Results of this model show that the existence of the porous substrate may improve the Nusselt number at the fully developed region by a factor of 8. However, there is an optimum thickness of the porous substrate beyond which no significant improvement in the Nusselt number is achieved. Teamah and Shoukri (1995) treated a similar phenomenon to determine the effect of radius ratio, aspect ratio and buoyancy ratio on the double diffusive natural convection in vertical annulus enclosures. The ranges of the

parameters being studied were 1-5 for radius ratio, 1-4 for the aspect ratio and 10^{-3} to 10^{+3} for buoyancy ratio.

Mixed heat transfer in a horizontal rotating annulus with thermal driven flows only was initially studied numerically by Lee (1984) and Fusegi *et al.* (1986). Recently, Yoo (1998a, 1998b, 1999a, 1999b) conducted a series of numerical studies for a horizontal rotating annulus. These studies cover a wide range of Grashof and Prandtl numbers. Islam *et al.* (2001) presented experimental and numerical investigations on the steady laminar mixed-convection heat transfer in a horizontal concentric annulus by using air and water. The cylinder is made of steel sheet with an outer diameter of 38.1 mm, a length of 1 m and a thickness of 1mm. The coupled governing equations are numerically solved over the range of conditions as $10^4 \leq Ra \leq 10^8$, $0.7 \leq Pr \leq 5.42$ and $200 \leq Re \leq 1000$. When the fluid moved from the entrance, the buoyancy forces became stronger and affected the temperature field at the upper half, which caused a noticeable distortion. The results were influenced by the effect of Rayleigh number on the secondary flow, axial velocity profile, heat transfer and pressure drop. Increasing the Prandtl number decreased the Nusselt number, and the predicted Nusselt number was compared with the experimental results. Nusselt number first decreased rapidly after a certain distance and then gradually increased before remaining uniform. The secondary flow was more intense in the upper pan than in the lower pan and increased throughout the cross-section until the intensity reached a maximum value. Teamah *et al.* (2005) studied the same geometry used by Yoo (1998a, 1998b) with different parametric study for rotational Reynolds number, radius ratio and Prandtl number. They studied the transitions in flow from no cells to one cell and from one cell to two cells. Shi and Lu (2005, 2006) investigated the double-diffusive natural convection in a vertical cylinder with radial temperature and axial solutal gradients; they aimed to understand the effect of the buoyancy ratio on the evolution of the flow field, temperature and solute field in the cavity. Sung *et al.* (1993) studied numerically convection double diffusive in a rotating horizontal annulus, where Neumann boundary conditions are adopted, the external temperature gradient is imposed horizontally, whereas the solutal gradient is applied in the vertical direction. The effect of the rotation in a double-diffusive convection for a stably stratified fluid within an annulus is investigated by Lee *et al.* (1999, 2000). They have demonstrated the effect of rotation on the development and merging of the multi-layered flow structure and various field variables.

In recent years, the paper presented by Jha *et al.* (2015) derives analytical solutions of fully developed natural convection heat and mass transfer in a vertical annular non-Darcy porous medium. This investigation concerned the situation, where Soret effect is present, and the flow is both aided and opposed. The influence of the controlling parameters on the flow characteristics has been seen to be higher for double diffusion in the absence of Soret effect than in the presence of Soret effect. It is found that the presence of Soret effect reduces the dependence of the volume flow rate. Numerical study of double diffusive buoyancy forces induced natural convection in a trapezoidal enclosure partially heated from the right sidewall is investigated by Gholizadeh *et al.* (2016). The numerical results are reported for the effect of different heating cases, thermal Grashof numbers and inclination angles on the contours of streamline, temperature and concentration. Also, the relevant results for the average Nusselt and Sherwood numbers are demonstrated for several parameters including thermal Grashof number, Lewis number, Prandtl number at a fixed aspect ratio and buoyancy ratio.

2. Mathematical formulation

2.1 Physical model

Figure 1, shows the geometry of the considered problem in the coordinates system. Consider two long concentric horizontal cylinders with gap width d, partially filled with a homogeneous isotropic porous medium. The inner cylinder of radius r_i and the outer cylinder of radius r_0 are kept at uniform temperatures T_i and T_0 and concentrations C_i and C_0, respectively, with $T_i > T_0$ and $C_i > C_0$ for aiding case or $C_i < C_0$ for opposing case. The inner cylinder is fixed, whereas the outer cooled cylinder is kept on rotating in the counter-clockwise direction with a constant angular velocity ω. The flow in the annular region is assumed to be three-dimensional, steady and laminar. Also, all thermo-physical properties of the fluid are considered constant except for the density variation in the buoyancy term, where the Boussinesq approximation is considered.

The density at the reference temperature, thermal and concentration expansions respectively are written as follows:

$$\rho = \rho_0[1 - \beta_T(T - T_0) - \beta_S(C - C_0)] \tag{1}$$

$$\beta_T = -\frac{1}{\rho_0}\left(\frac{\partial \rho}{\partial T}\right)_{P,C} \text{ and } \beta_S = -\frac{1}{\rho_0}\left(\frac{\partial \rho}{\partial C}\right)_{P,T} \tag{2}$$

2.2 Governing equations

For purposes of solving the governing equations in the dimensionless form, the following dimensionless variables are introduced to the governing equations:

$$(Z, R) = (z, r)/d; (V_r, V_z, V_\varphi) = (v_r, v_z, v_\varphi)/(\Omega.r_0); C = \frac{c - c_0}{c_i - c_0};$$

$$\omega = \frac{\Omega(r_0 - r_i)}{\Omega r_0}\theta = \frac{T - T_0}{T_i - T_0}; P = \frac{P}{\rho\left(\frac{\Omega r_0}{\varepsilon}\right)^2} \tag{3}$$

The dimensionless governing equations for the conservation of mass, momentum, heat and solute concentration in a porous medium annulus are given by:

$$\nabla \cdot u = 0 \tag{4}$$

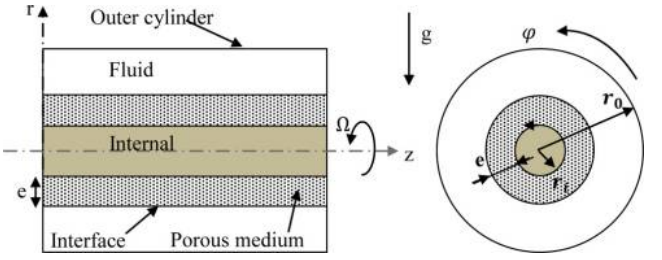

Figure 1.
Problem configuration

$$\left[V_z\frac{\partial V_r}{\partial z}+V_r\frac{\partial V_r}{\partial R}+V_z\frac{\partial V_\varphi}{R}\right]=-\frac{\partial p}{\partial R}+\frac{\varepsilon R_\mu}{R_e}\left[\nabla^2 V_r-\frac{V_r}{R^2}-\frac{2}{R^2}\frac{\partial V_\varphi}{\partial_\varphi}\right]$$
$$-\frac{\varepsilon^2 Gr_T}{R_e^2}[\theta+NC]-\left(\frac{\varepsilon}{R_e D_a}V_r+C_1\frac{C_F}{\sqrt{D_a}}\sqrt{V_r^2+V_z^2+V_\varphi^2}V_r\right) \quad (5)$$

$$\left[V_z\frac{\partial V_z}{\partial z}+V_r\frac{\partial V_z}{\partial R}+\frac{V_\varphi}{R}\frac{\partial V_z}{\partial \varphi}\right]=-\frac{\partial p}{\partial z}+\frac{\varepsilon R_\mu}{R_e}[\nabla^2 V_z]$$
$$-\left(\frac{\varepsilon}{R_e D_a}V_z+C_1\frac{C_F}{\sqrt{D_a}}\sqrt{V_r^2+V_z^2+V_\varphi^2}V_r\right) \quad (6)$$

$$\left[V_z\frac{\partial V_\varphi}{\partial z}+V_r\frac{\partial V_\varphi}{\partial r}+\frac{V_\varphi}{R}\frac{\partial V_\varphi}{\partial \varphi}+\frac{V_r V_\varphi}{R}\right]=+\frac{\varepsilon R_\mu}{R_e}\left[\nabla^2 V_\varphi-\frac{V_\varphi}{R}+\frac{2}{R^2}\frac{\partial V_r}{\partial \varphi}\right]$$
$$-\left(\frac{\varepsilon}{R_e D_a}V_\varphi+C_1\frac{C_F}{\sqrt{D_a}}\sqrt{V_r^2+V_z^2+V_\varphi^2}V_\varphi\right) \quad (7)$$

$$\left(V_r\frac{\partial \theta}{\partial R}+V_z\frac{\partial \theta}{\partial z}+\frac{V_\varphi}{R}\frac{\partial \theta}{\partial \varphi}\right)=\frac{R_\alpha}{R_e P_r}\left(\frac{\partial^2\theta}{\partial R^2}+\frac{1}{R}\frac{\partial \theta}{\partial R}+\frac{1}{R^2}\frac{\partial^2\theta}{\partial \varphi^2}+\frac{\partial^2\theta}{\partial z^2}\right) \quad (8)$$

$$\left(V_r\frac{\partial C}{\partial R}+V_z\frac{\partial C}{\partial z}+\frac{V_\varphi}{R}\frac{\partial C}{\partial \varphi}\right)=\frac{R_D}{R_e S_c}\left(\frac{\partial^2 C}{\partial R^2}+\frac{1}{R}\frac{\partial C}{\partial R}+\frac{1}{R^2}\frac{\partial^2 C}{\partial \varphi^2}+\frac{\partial^2 C}{\partial z^2}\right) \quad (9)$$

In equations (5-7), the coefficient C_1 can be set equal 0 or 1 to obtain the Darcy–Brinkman or Darcy–Brinkman–Forchheimer models. The dimensionless parameters governing double-diffusive mixed convection in the porous annulus are the thermal Grashof number Gr_T, the rotational Reynolds number Re, the Darcy number Da, the Lewis number Le, the Prandtl number Pr, the Buoyancy ratio N, kinematic viscosity ratio R_μ, mass diffusivity ratio R_D and thermal conductivity ratio R_λ, defined by:

$$Gr_T=\frac{g\beta_T d^3(T_0-T_i)}{\nu^2}, R_e=\frac{\Omega R_0 d}{\gamma}, Da=\frac{k}{d^2}, Le=\frac{\alpha}{D}, Pr=\frac{\gamma}{\alpha}, N=\frac{\beta_S\Delta C}{\beta_T\Delta T},$$
$$R_\mu=\frac{\mu_{eff}}{\mu}, R_D=\frac{D_{eff}}{D}, R_\lambda=\frac{\lambda_{eff}}{\lambda} \quad (10)$$

In addition to the above dimensionless parameters, the present study also involves the geometrical parameters, such as the radius ratio η and the aspect ratio A, given by:

$$\eta=\frac{r_i}{r_o}, A=\frac{z}{d} \quad (11)$$

The dimensionless boundary conditions are:

$$V_r = V_z = V_\varphi = 0, \quad C = \theta = 1 \qquad \text{at } (R = R_i, Z, \varphi)$$

$$V_r = V_z = 0, \; V_\varphi = 1 \quad C = \theta = 0 \qquad \text{at } (R = R_0, Z, \varphi)$$

$$V_r = V_\varphi = V_z = 0 \quad C = \theta = 0 \qquad \text{at } (R, Z = Z_{inl}, \varphi)$$

$$\frac{\partial V_r}{\partial Z} = \frac{\partial V_z}{\partial Z} = \frac{\partial V_\varphi}{\partial Z} = \frac{\partial \theta}{\partial Z} = \frac{\partial C}{\partial Z} = 0 \quad \text{at } (R, Z_{out}, \varphi) \tag{12}$$

The local Nusselt (Nu), average Nusselt (Nu_φ), local Sherwood (Sh) and average Sherwood numbers (Sh_φ) along the outer cylinder are defined, respectively, by:

$$Nu = \ln\left(\frac{R_i}{R_0}\right)\left(R\frac{\partial \theta}{\partial R}\right)_{R_0}, Nu_\varphi = \frac{1}{2\pi}\int_0^{2\pi} Nu \, d\varphi,$$

$$Sh = \ln\left(\frac{R_i}{R_0}\right)\left(R\frac{\partial C}{\partial R}\right)_{R_0}, Sh_\varphi = \frac{1}{2\pi}\int_0^{2\pi} Sh \, d\varphi \tag{13}$$

The dimensionless stream function ψ is calculated by integrating the dimensionless velocity in the angular direction as follows:

$$\psi = \int_{R_i}^{R} (-V_\varphi) dR \tag{14}$$

3. Numerical procedure

The governing equations of Navier–Stokes, energy and mass are discretized on a non-uniform cylindrical grid using a finite volume approach developed by Patankar (1980). This technique was based on the discretization of the governing equations using the central differencing in space. The numerical grid of ($80 \times 50 \times 25$) was adopted in this work and the residuals of momentum, energy and solutal equations are all less than 10^{-6}.

To calculate both Nusselt and Sherwood numbers, we use numerical differentiations, $(\partial\theta/\partial R)_{R=R_i}$ and $(\partial\theta/\partial R) = \lim_{\Delta R \to 0} \partial\theta/\partial R$. Therefore, at the cylinder wall, we need very fine grids to obtain accurate results. Particularly in the region close to the walls and also in the region in the vicinity of the annular space inlet, we use a power law to generate the grid radially, and this law is given by the expression $R_j = 1 - 0.5[(n - J)/n]^{0.5}$. Regarding the axial direction, we propose a grid evolving according to a series geometric reason 1.1 which is written as follows $\Delta X_{i+1} = 1.0X_i$. In φ direction, we do not need numerical differentiations. Therefore, a uniform grid was taken in this direction. The iteration method used in this program is a line-by-line procedure, which is a combination of the direct method and the resulting Tri Diagonal Matrix Algorithm. The accuracy was defined by the change in the average Nusselt and the other dependent variables through 100 iterations to be less 0.02 per cent from its value. The check showed that 3,500 iterations were enough for all of the study values.

4. Code validation and comparison with previous works

The numerical technique implemented in the present study has been successfully used in our recent papers to investigate the effects of porous portion of the thermal and mass transfer. However, to verify the accuracy of the current numerical results, simulations of the present model are tested and compared with different reference solutions available in the literature for thermo-solutal convection in the cylinder annular. Therefore, a computer program was constructed in a general form to solve most parameters affecting the double diffusive mixed convection in rotating annulus. The program was run when the outer cylinder was rotating. The dimensionless temperature and concentration at the inner cylinder were kept constant and their values equal one, whereas their values at the outer cylinder equal zero for the aiding case, in the opposing case, the concentration at the outer cylinder equal one, and it will be zero at the inner cylinder. These conditions were the same as those studied by Al-Amiri and Khanafer (2006).

Figure 2 shows both the average Nusselt and Sherwood numbers over a range of buoyancy ration from −12 to +12. The results for Lewis number was kept constant at one, the thermal Rayleigh number at 10^4, Prandtl number at 0.7 and rotational Reynolds number as 100. It can be seen from this figure that the solution of the present numerical code is in excellent agreement with the results of Al-Amiri and Khanafer (2006).

A second comparison was made to validate the numerical code with the results obtained by Khanafer and Chamkha (2003); in this case, annular space is completely filled by a porous medium and for the conditions themselves. Figure 3 exhibits a good agreement between the present results and those of Khanafer and Chamkha (2003) for various Rayleigh numbers.

5. Results and discussion

The numerical results are presented in this section with the main objective of investigating the effect of the heat and solute transfer source location and buoyancy ratio on the double-diffusive convection flow and the corresponding heat and mass transfer rates in a horizontal porous annulus. Because the present study involves a large number of non-dimensional parameters (Gr_T, Gr_S, Da, Pr, Sc, Re, R_D, R_μ, R_λ, C_F, ω, N, ε), only the main controlling

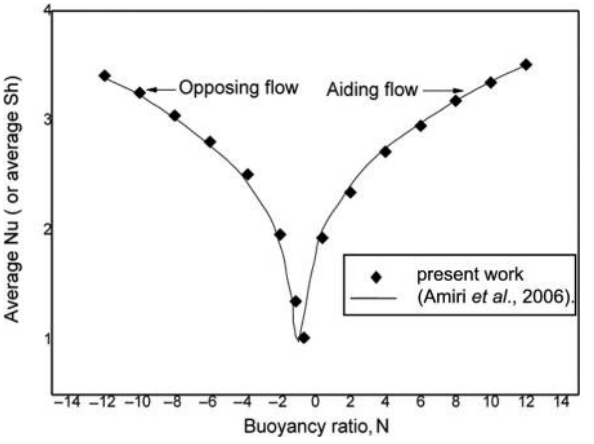

Figure 2. Comparisons of buoyancy ratio number on the average Nusselt number (or Sherwood number) between the present work and that of (Al-Amiri and Khanafer, 2006), for Ra = 104, Re = 100, Le = 1, Pr = 0.7 and $\eta = 0.5$

parameters are varied. The aspect ratio (A) of the annulus, Prandtl number (Pr), Schmith number (Sc) and porosity of the porous medium (ε) are kept, respectively, at 150, 0.71, 0.65 and 0.4. Furthermore, the Forchheimer coefficient (C_F) is fixed at 100; however, it's located (Da) is varied from 10^{-1} to 10^{-6}, the thermal Grashof number (Gr_T), solutal Grashof number (Gr_S) are varied in the range [10^3, 10^6]. Curvature effect can be important for the annular cavity flows and so the effect of rotation speed (ω) on the temperature profile is also examined for a wide range ($0 \leq \omega \leq 10$).

The relative importance of thermal and solutal buoyancy forces is denoted by the ratio (N) and is defined as the ratio of the solutal buoyancy force to thermal buoyancy force. This parameter is varied through a wide range corresponding to ($-50 \leq N \leq +50$), covering the concentration-dominated opposing flow (N = −50), pure convection-dominated flow (N = 0) and concentration-dominated aiding flow (N = +50). In the following sections, the flow fields, temperature and concentration distributions in the fluid and porous annulus are illustrated through streamlines, isotherms and isoconcentrations. In all graphs, the left and right vertical axes correspond to the inner and outer cylinders, respectively.

5.1 Effect of the buoyancy ratio number

In the mixed convection system, the forced flow can aid or oppose the buoyancy induced flow. In the present configuration, both aiding and opposing effects exist. The distribution of axial and radial velocities at $z = 61.75$ are presented in Figure 4(a) and (b) for N = 0, +2, +4, +8, +10 and −1, −2, −4, −8, −10, with Da = 10^{-2} and e = 0.4. When the buoyancy forces are applied in the same way, these figures show that the velocity component $V_r(r)$ decreases with decreasing of N in the porous medium, whereas in the fluid zone near the colder wall ($r = r_0$), the flow is reversed. Concerning the axial velocity component $V_z(r)$, it always takes positive values under the action of the input speed, but it reverses for negative values of the buoyancy ratio N. Furthermore, the interesting behavior of the reversed flow occurs at N = −10 [Figure 4(b)], where a reversing flow is found in both fluid and porous mediums. This phenomenon is because of the effect of solutal gradient which plays a destabilizing role of the flow.

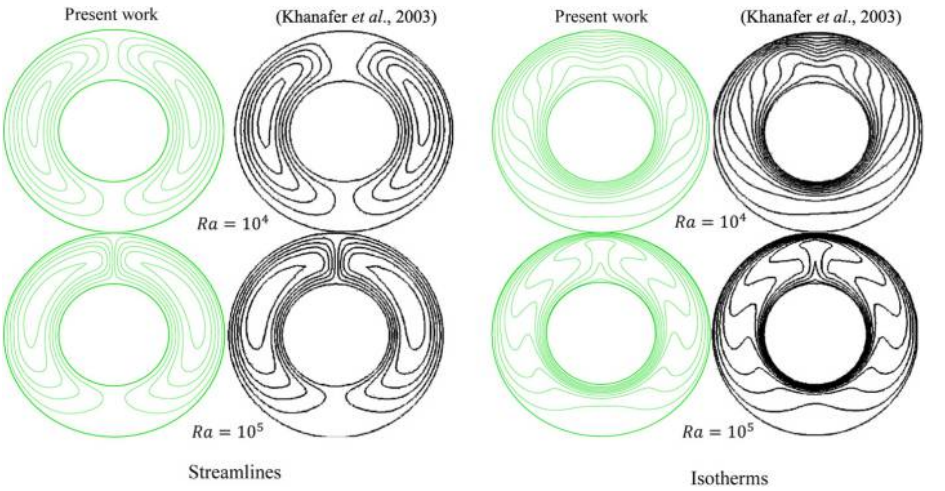

Figure 3.
Comparisons of the streamlines and isotherms between the present work and that of Khanafer and Chamkha (2003), for Da = 10^{-1}, Re = 10, F = 0.1, ε = 0.97 and η = 0.5 in a porous horizontal cylindrical annulus

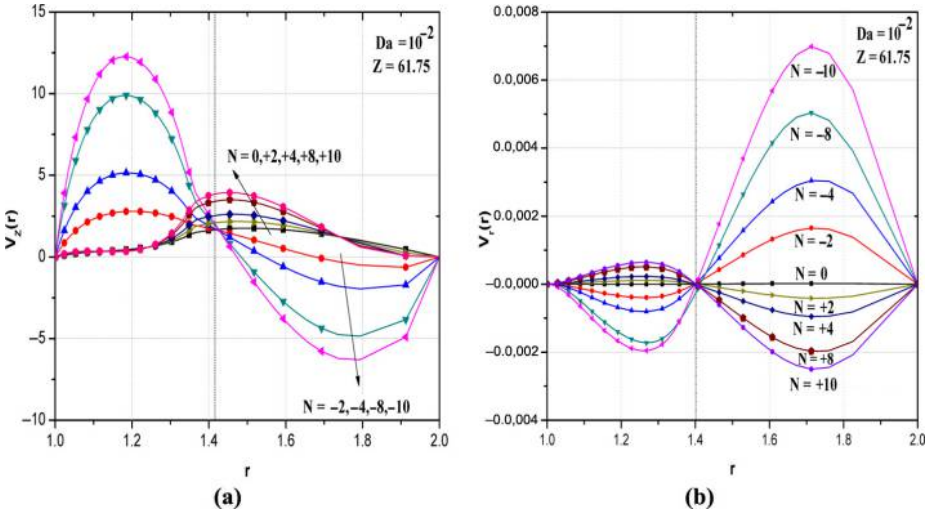

Figure 4.
Effect of the buoyancy ratio number on the radial profile of axial and radial velocities for (a) $N > 0$, (b) $N < 0$

In this section, we are interested in the effect of buoyancy ratio number on the flow structure and the heat and mass transfers, in both cases, aiding and opposing double diffusive convection for equal thermal and solutal diffusivities when all the annular space is filled by a porous medium. Figures 5 and 6 show the streamlines (a), the isotherms (b) and isoconcentrations (c) for the case $Gr_T = 10^3$, $Pr = 0.71$, $Sc = 0.67$, $R = 2$, $\varepsilon = 0.4$, $Da = 10^{-2}$. A tricellular flow exists in the two halves of the annulus when the effects of solutal convection on thermal convection is weak (for smaller values of N); two cells are at the top of the inner cylinder and four others are positioned laterally on both right and left sides of the annular space. In fact, as N is increased, the flow rate decreases and the flow structure becomes bicellular, the side cell center moves upwards and the maximum of the current function ψ_{max} is decreasing.

For high values of the buoyancy ratio ($N > +20$), an intense temperature gradient is located at the bottom of the hot inner cylinder and up the cold outer cylinder (same remark for solutal gradient). It also appears that a single cell flow ascending the side of the inner cylinder and down the side of the outer cylinder ($N = \pm 50$), which means that the buoyancy forces induced by the solute effect stabilize the flow structure.

When the inner cylinder is kept at a constant concentration (opposite case), it is found that all the qualitative characteristics of the flow will be the same as for $N > 0$, but the flow directions are reversed with a relative symmetry to the axis of the two cylinders. Figure 6 shows the plot of the streamlines, the isotherms and iso-concentrations for this case.

5.2 Effect of Darcy number and rotation velocity

The effects of the Darcy number and the rotation speed on the radial temperature are presented in Figure 7. It is noted that the rotation velocity greatly reduces the temperature in the annular space, indicating that the heat transfer is disadvantaged by the rotation velocity. This behavior is more accentuated as Darcy number values increase ($D_a > 10^{-2}$). For a given value of the rotation velocity, it is found that the temperature decreases as the Darcy

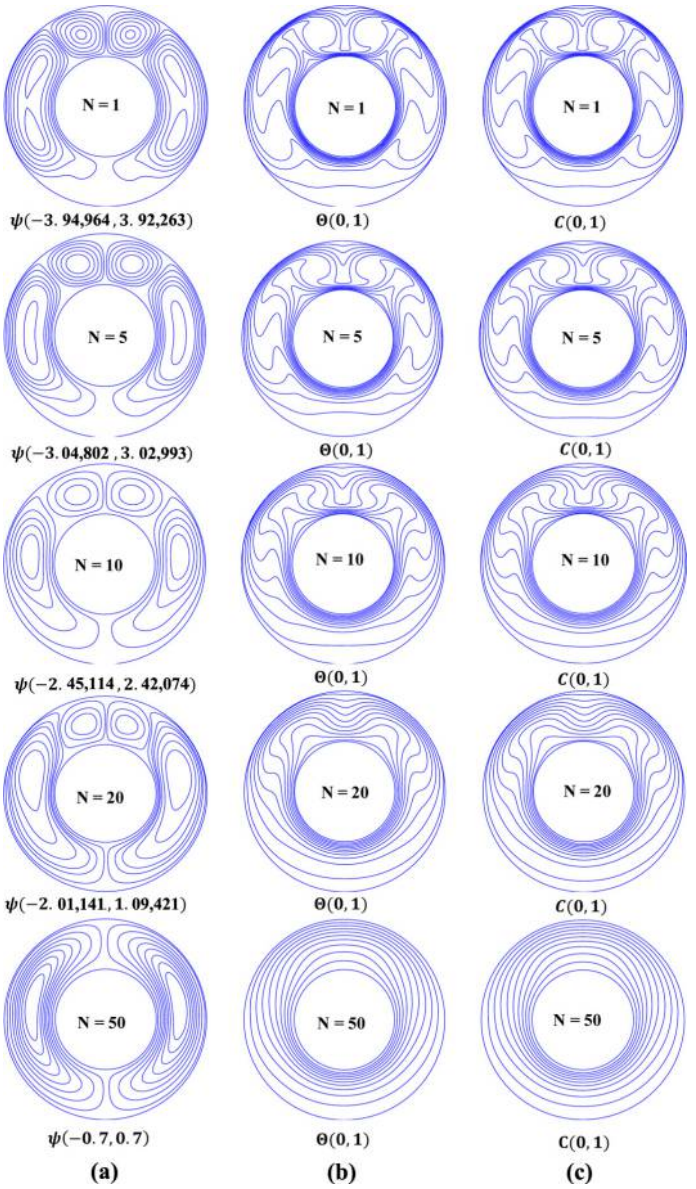

Figure 5.
Effect of the positive buoyancy ratio number on the streamlines, isotherms and ISO concentrations for $Gr_T = 10^3$, Pr = 0.71, Sc = 0.67, Z = 75.5, R = 2, $\varepsilon = 0.4$, $Da = 10^{-2}$, $R_\alpha = 10$, $R_D = 10$

number up to $D_a = 10^{-5}$, where all radial profiles coincide and the temperature becomes almost the same for all ω values.

Figures 8(a)-(d) illustrate the effect of the rotational speed on the radial profile of the axial component velocity for different Darcy numbers in an annular space filled to 40 per cent of a porous layer of side of the inner wall. In all the figures, it is observed

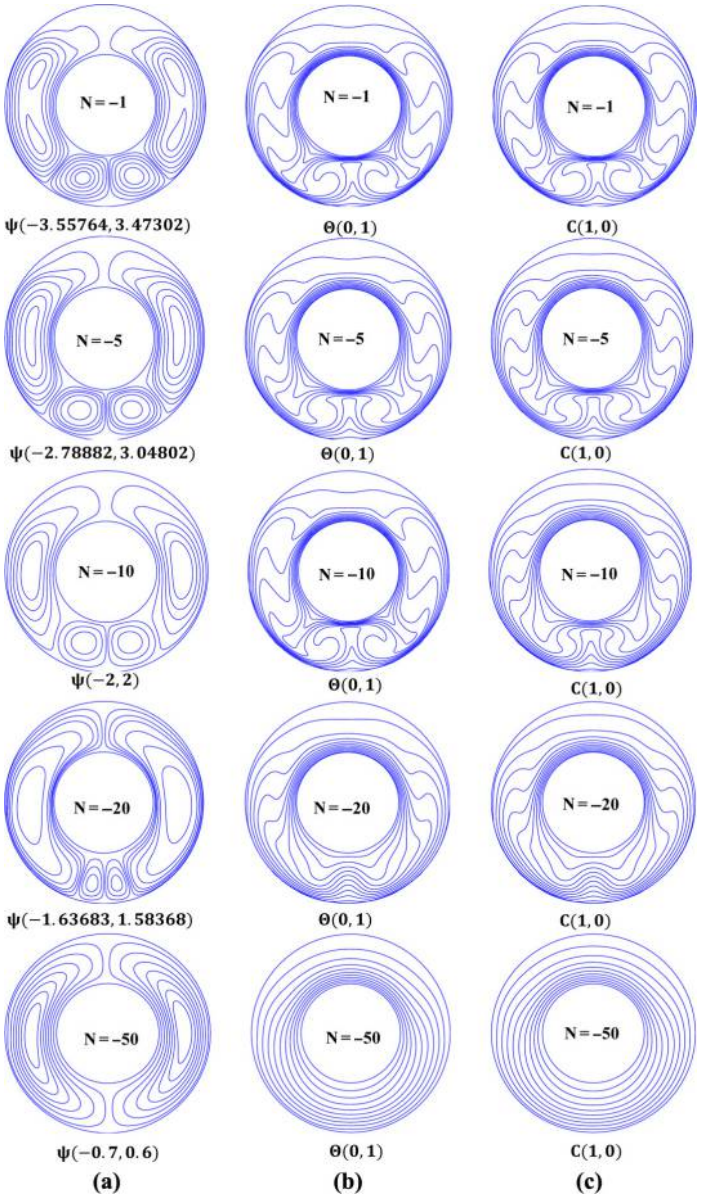

Figure 6.
Effect of the negative buoyancy ratio number on the streamlines (a), isotherms (b) and ISO concentrations (c) for $Gr_T = 10^3$, Pr = 0.71, Sc = 0.67, Z = 75.5, R = 2, $\varepsilon = 0.4$, Da = 10^{-2}, $R_\alpha = 10$, $R_D = 10$

that the values of axial velocity decrease when the rotational speed increases; this is true for the fluid area, whereas in the porous area, we note two distinct parts, one close to the interface complies with the same behavior as the fluid area, whereas the other one is the reverse phenomenon which occurs. The widths of the two parts are according to the Darcy number. Indeed, for large values of Darcy number, the area situated on the

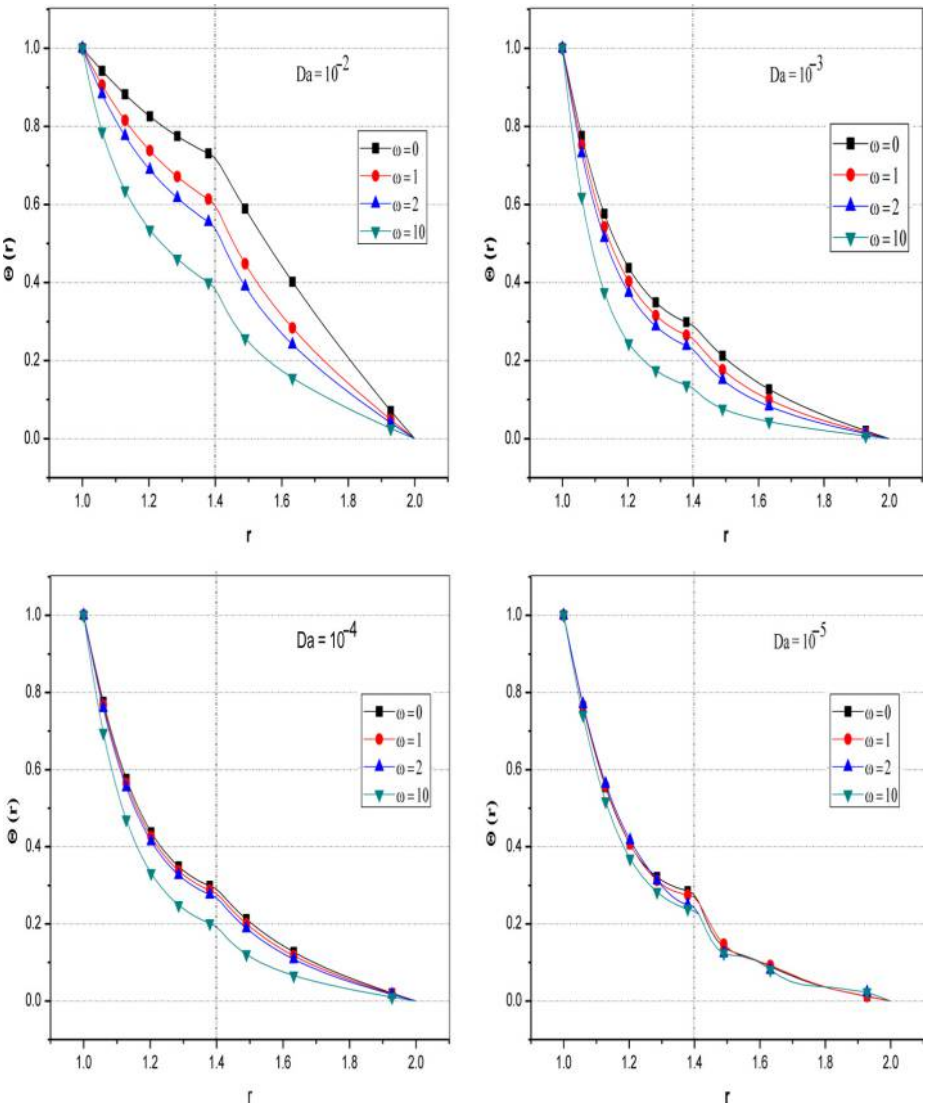

Figure 7.
Radial temperature profile for different values of rotational velocity and Darcy number for Pr = 0.71, e = 0.4, C_F = 100, Re = 100, $Gr_T = 10^{+5}$, $Gr_s = 10^{+5}$

side of the rotating cylinder is less important than the second, whereas for small values of Darcy number, the first area takes the scale and the second tends to disappear for some values of ω when Da = 10^{-3}. For Da = 10^{-4} and in the same porous area, we note that all axial velocity curves coincide and indicate a velocity near zero, which confirms that the fluid does not penetrate into this region when the pores become very small. Figure 8(a) shows that from the value of $\omega = 4$, the maximum of the axial velocity starts to move toward the inner cylinder under the rotation effect. These curves also show that the axial velocity drops by half when the Darcy number varies between 10^{-1} and 10^{-4}.

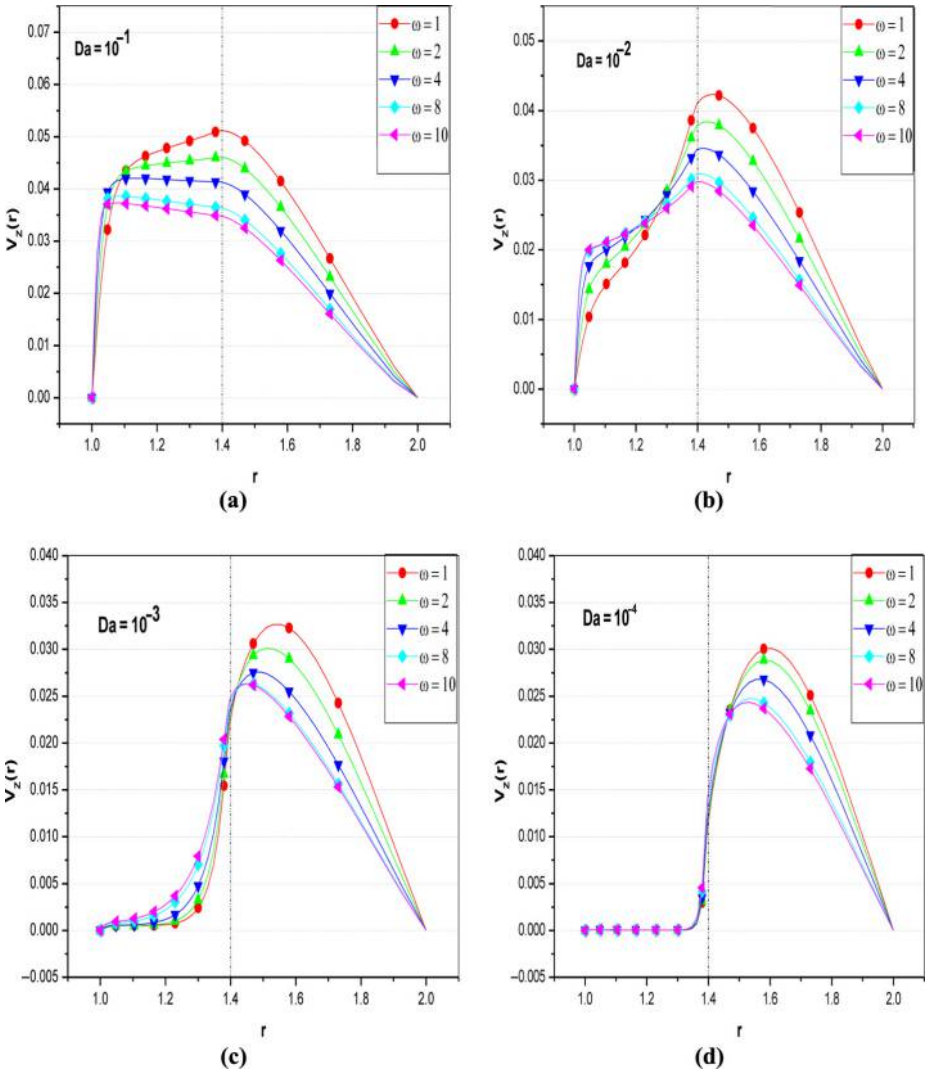

Figure 8.
(a)-(d) Effect of the rotational velocity on the radial profile of the axial component velocity for different Darcy, Pr = 0.71, e = 0.4, Re = 100, C_F = 100, $Gr_T = 10^{+5}$, $Gr_s = 10^{+5}$

Figure 9 shows the distribution of the radial velocity in a given section (Z = 1.073) for a Darcy number Da = 10^{-2} and different rotational velocity values. In the porous region, the radial velocity of fluid decreases with increasing rotational velocity and takes negative values, as can be seen from ω = 1 to 10, which leads to the appearance of a fluid recirculation cell in round of this axial position that influences the evolution of fluid temperature near the inner wall.

This behavior of the radial velocity continues in the fluid zone, where it is noted that the velocity has increasingly negative values in particularly for low values of the rotational speed ($0 \geq \omega \geq 1$), when the radial profile cancels in the rest of the area. However, when ω varies between 1 and 10, a small decrease is observed.

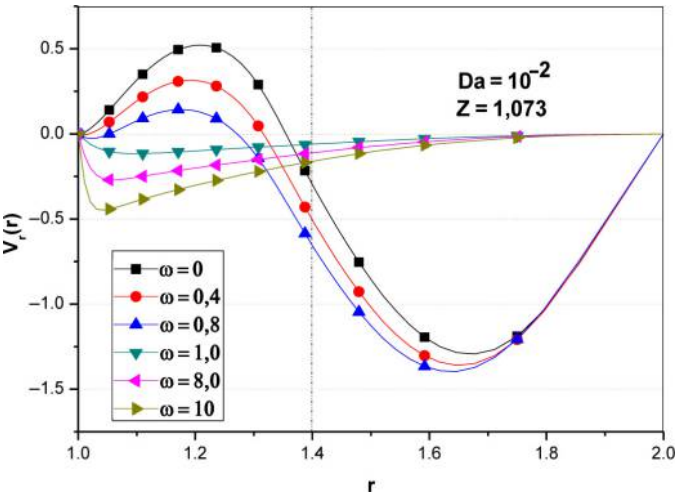

Figure 9.
Variation of the radial velocity for different rotational velocity values, Pr = 0.71, e = 0.4, $C_F = 100$, $Gr_T = 10^{+5}$, $Gr_s = 10^{+5}$

5.3 Effect of position

The radial profiles of the axial velocity component for different positions along the pipe are shown in Figure 10 when the porous matrix fills 20 per cent of the annulus. In the porous layer, we observe that there is no fluid flow (Da = 10^{-6}), whereas the velocity profile takes a parabolic Poiseuille curvature within the fluid area. More that goes downstream of the cylinder more that the axial velocity component increases and the regime becomes stabilized.

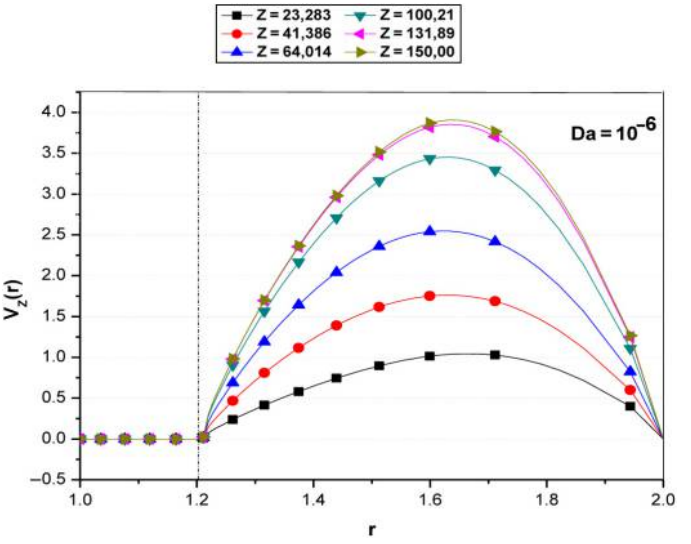

Figure 10.
Distribution of the axial component of velocity for different positions for pr = 0.71, da = 10^{-6}, e = 0.4, $C_F = 100$, $Gr_T = 10^{+5}$, $Gr_s = 10^{+5}$

5.4 Effect of thermal conductivity ratio

To have a better understanding of the curvature effects on the convective heat transfer in both porous and fluid annulus, the average temperature along the mid-section of the annular space is depicted in Figure 11 for three different values of Richardson number corresponding to three convection modes. An overview of the figure reveals that the average temperature decreases with the Richardson number for boundary layer on the both inner and outer walls. For low values of thermal conductivity ratio, the average temperature curve rises slightly to $R_\lambda = 100$ and then remains almost flat beyond this value. This function can be attributed to the existence of a delay in a thin thermal boundary layer which is adjacent to the both of the annulus space walls.

In Figure 12, variations of average Nusselt number on inner surface depending on the thermal Grashof number are shown for different thermal conductivity ratios. It can be seen from this figure that the average Nusselt number on the inner cylinder decreases with increasing of the thermal conductivity ratio. We also find that for Grashof numbers less than or equal to 10^{+4}, whereas the Nusselt number is almost constant for each value of the thermal conductivity ratio R_λ, and, for higher values to 10^{+5}, we note that the heat transfer is favored by the Grashof number, especially for the case of a thermal conductivity ratio $R_\lambda = 1$, where the Nusselt number rises quickly with respect to the other two cases.

Figures 13(a)-(c) illustrate the effect of the thermal conductivity ratio R_λ on the dynamic, thermal and solutal fields, respectively. These numerical simulations are presented for the opposite case corresponding to $N = -1$ for a mass conductivity ratio equal to 1. The results show the appearance of two contra-rotating cells in both sides of the annular space, this is for $R_\lambda = 1$. Isothermal and isoconcentrations lines are distorted and not orthogonal to the walls of the two cylinders. These findings are similar to those of Tan and Howell (1989) in the case of a rectangular enclosure with two isothermal vertical walls and two adiabatic horizontal walls. It is found that when the thermal conductivity ratio R_λ is large, the center of the convective cell moves upward. It is also noted that the development of a small roller in the low speed region between the two base flow rollers occurs. Between the two rolls, a

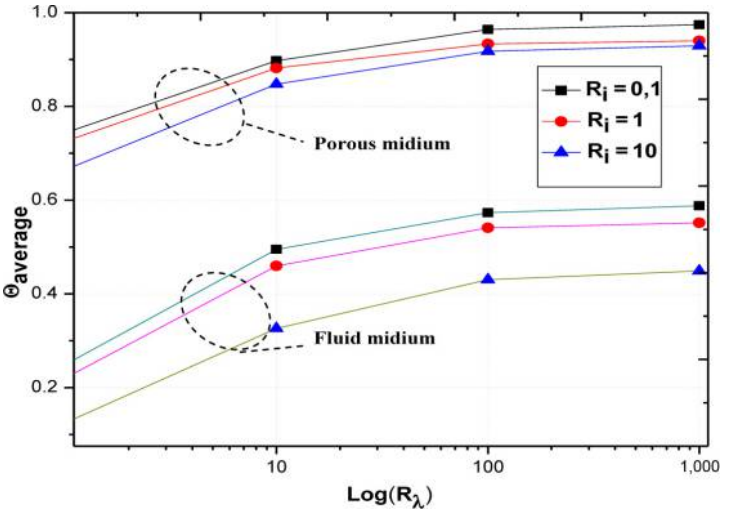

Figure 11.
Effect of thermal conductivity ratio on the average temperature profiles along Z = 75.5 for: $Da = 10^{-2}$, $Pr = 0.71$, $Gr_T = 10^{+5}$, $Gr_S = 10^{+5}$

stagnant zone extends gradually because of the presence of viscous forces when the R_λ increases. The secondary roller and those of base flow are co-rotating. Isothermal lines become less distorted in this case, more uniform in the angular direction until fit the shape of the walls in the immediate vicinity thereof. It means that the flow stability is improved by increasing of R_λ. In fact, for values corresponding to $Le > 10$, it is noted that the thermal diffusion coefficient is significantly higher than the mass diffusion coefficient, demonstrating that the thermal field is more affected than the concentration field by convective effects.

6. Conclusion

In the present work, we have numerically investigated the double-diffusive convection in a horizontal porous annulus when inner and outer walls are maintained at a constant temperature and concentration. The finite volume method was used to solve the set of governing equations using the SIMPLER algorithm. The effects of the main controlling parameters, such as buoyancy ratio, Darcy number, thermal and solutal Grashof numbers, the speed rotation and the thermal conductivity ratio were investigated in detail to gain new insights into the flow patterns, the thermal and the solutal fields and the rates of heat and mass transfer. Many of the observations of the present study are in good agreement with the similar studies in the literature. The main findings of the present investigation are summarized as follows:

- The flow structure, thermal and solutal fields, rates of heat and mass transfer are profoundly affected by the relative magnitudes of buoyancy ratio.
- When the solutal buoyancy forces are dominated ($N = -50$), the flow in the annulus is characterized by a single cell flow ascending the side of the inner cylinder and down the side of the outer cylinder. For smaller values of N, the fluid flow becomes multicellular.
- It is found that all the qualitative characteristics of the flow are the same for both cases $N > 0$ and $N < 0$, but the flow directions are reversed.

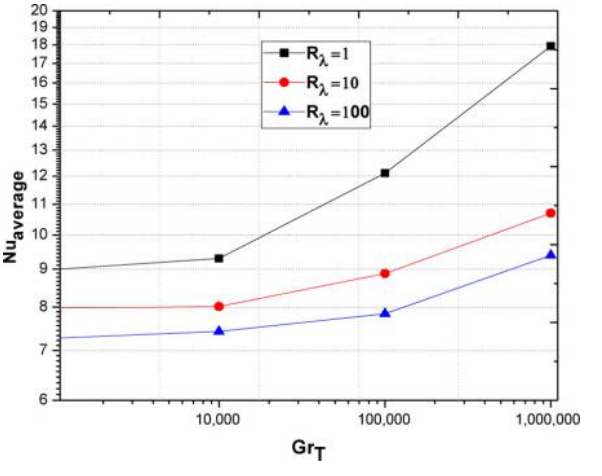

Figure 12.
Effect of the thermal Grashof number on the average Nusselt for different values of thermal conductivity ratio, $Re = 100$, $\varepsilon = 0.4$, $D_a = 10^{-3}$, $P_r = 0.71$ and $S_c = 0.7$

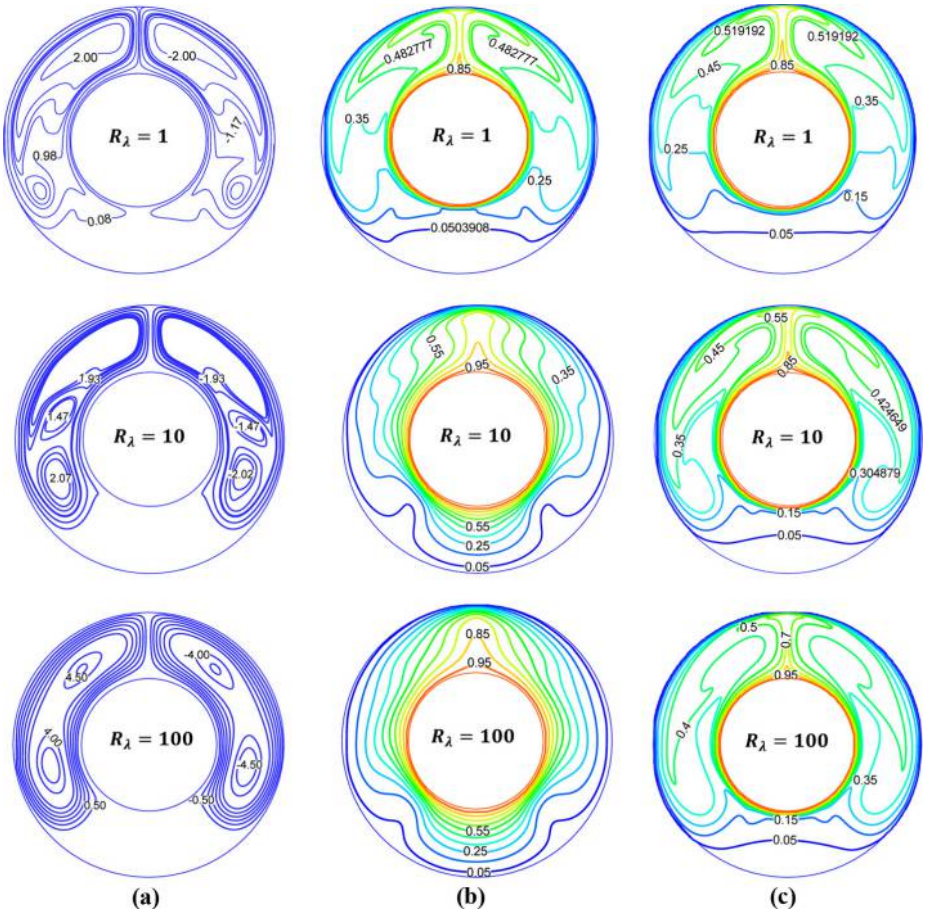

Figure 13.
Influence of the thermal conductivity ratio R_λ on the dynamic (a), thermal (b) and solutal field (c) when; N = −1, Re = 100, $\varepsilon = 0.4$, $D_a = 10^{-3}$, Z = 75.5, P_r = 0.7, S_c = 0.7 and R_D = 1

- In the porous medium, the velocity component $V_r(r)$ decreases with decreasing N, flow reversal is found in the fluid zone near the colder wall ($r = r_0$). The axial velocity component $V_z(r)$ always takes positive values under the action of the input speed, but it reverses for negative values of the buoyancy ratio N.
- The rotation speed greatly reduces the temperature in the annular space, this behavior is more accentuated as Darcy number values increase ($D_a > 10^{-2}$).
- The axial velocity drops by half when the Darcy number varies between 10^{-1} and 10^{-4}.
- The heat transfer is favored by the Grashof number, especially for the case of a thermal conductivity ratio $R_\lambda = 1$, where the Nusselt number rises quickly with respect to the other two cases.
- The thermal conductivity ratio significantly affects the heat transfer more than the mass transfer.

References

Aboubi, K., Robillard, L. and Vasseur, P. (1998), "Natural convection in horizontal annulus filled with an anisotropic porous medium", *International Journal of Numerical Methods for Heat & Fluid Flow*, Vol. 8 No. 6, pp. 689-702.

Al-Amiri, A.M. and Khanafer, K.M. (2006), "Numerical simulation of double diffusive mixed convection within a rotating horizontal annulus", *International Journal of Thermal Sciences*, Vol. 45 No. 6, pp. 567-578.

Aldoss, T.K., Alkam, M. and Shatarah, M. (2004), "Natural convection from a horizontal annulus partially filled with porous medium", *International Communications in Heat and Mass Transfer*, Vol. 31 No. 3, pp. 441-452.

Alkam, M.K. and Al-Nimr, M.A. (1998), "Transient non-darcian forced convection flow in a pipe partially filled with a porous material", *International Journal of Heat and Mass Transfer*, Vol. 41 No. 2, pp. 347-356.

Barbosa Mota, J.P. and Saatdjian, E. (1995), "Natural-convection in porous cylindrical annuli", *International Journal of Numerical Methods for Heat & Fluid Flow*, Vol. 5 No. 1, pp. 3-12.

Barbosa Mota, J.P.B. and Saatdjian, E. (1997), "On the reduction of natural convection heat transfer in horizontal eccentric annuli containing saturated porous media", *International Journal of Numerical Methods for Heat & Fluid Flow*, Vol. 7 No. 4, pp. 401-416.

Benzeghiba, M., Chikh, S. and Campo, A. (2003), "Thermosolutal convection in a partly porous vertical annular cavity", *Journal of Heat Transfer: Transactions of the ASME*, Vol. 125 No. 4, pp. 703-715.

Char, M.-I. and Lee, G.-C. (1998), "Maximum density effects on natural convection in a vertical annulus filled with a non-darcy porous medium", *Acta Mechanica*, Vol. 128 Nos 3/4, pp. 217-231.

Fusegi, T., Farouk, B. and Ball, K.S. (1986), "Mixed-convection flows within a horizontal concentric annulus with a heated rotating inner cylinder", *Numerical Heat Transfer*, Vol. 9 No. 5, pp. 591-604.

Gholizadeh, M.M., Nikbakhti, R., Khodakhah, J. and Ghasemi, A. (2016), "Numerical study of double diffusive buoyancy forces induced natural convection in a trapezoidal enclosure partially heated from the right sidewall", *Alexandria Engineering Journal*, Vol. 55 No. 2, pp. 779-795.

Havstad, M.A. and Burns, P.J. (1982), "Convective heat transfer in vertical cylindrical annuli filled with a porous medium", *International Journal of Heat and Mass Transfer*, Vol. 25 No. 11, pp. 1755-1766.

Islam, N., Gaitonde, U.N. and Sharma, G.K. (2001), "Mixed convection heat transfer in the entrance region of horizontal annuli", *International Journal of Heat and Mass Transfer*, Vol. 44 No. 11, pp. 2107-2120.

Jha, B.K. (2005), "Free-convection flow through an annular porous medium", *Heat Mass Transfer*, Vol. 41 No. 8, pp. 675-679.

Jha, B.K., Joseph, S.B. and Ajibade, A.O. (2015), "Role of thermal diffusion on double-diffusive natural convection in a vertical annular porous medium", *Ain Shams Engineering Journal*, Vol. 6 No. 2, pp. 629-637.

Khanafer, K. and Chamkha, A.J. (2003), "Mixed convection within a porous heat generating horizontal annulus", *International Journal of Heat and Mass Transfer*, Vol. 46 No. 10, pp. 1725-1735.

Khanafer, K., Al-Amiri, A. and Pop, I. (2008), "Numerical analysis of natural convection heat transfer in a horizontal annulus partially filled with a fluid-saturated porous substrate", *International Journal of Heat and Mass Transfer*, Vol. 51 No. 7, pp. 1613-1627.

Kumari, M. and Nath, G. (2008), "Unsteady natural convection from a horizontal annulus filled with a porous medium", *International Journal of Heat and Mass Transfer*, Vol. 51 No. 19, pp. 5001-5007.

Lee, J., Kang, S.H. and Son, Y.S. (1999), "Experimental study of double-diffusive convection in a rotating annulus with lateral heating", *International Journal of Heat and Mass Transfer*, Vol. 42 No. 5, pp. 821-832.

Lee, J., Kang, S.H. and Son, Y.S. (2000), "Numerical study of multi-layered flow regime in double-diffusive convection in a rotating annulus with lateral heating", *Numerical Heat Transfer, Part A*, Vol. 38 No. 5, pp. 467-489.

Lee, T.S. (1984), "Numerical experiments with laminar fluid convection between concentric and eccentric heated rotating cylinder", *Numerical Heat Transfer*, Vol. 7 No. 1, pp. 77-87.

Mohamad, A.A. (2003), "Heat transfer enhancements in heat exchangers fitted with porous media part I: constant wall temperature", *International Journal of Thermal Sciences*, Vol. 42 No. 4, pp. 385-395.

Nield, D.A. and Bejan, A. (2006), *Convection in Porous Media*, 3rd ed., Springer, New York, NY.

Padilla, E.L.M. and Silveira-Neto, A. (2008), "Large-eddy simulation of transition to turbulence in natural convection in a horizontal annular cavity", *International Journal of Heat and Mass Transfer*, Vol. 51 No. 13, pp. 3656-3668.

Patankar, S.V. (1980), *Numerical Heat Transfer and Fluid Flow*, Mc-Graw Hill, New York, NY.

Pavel, B.I. and Mohamad, A.A. (2004), "An experimental and numerical study on heat transfer enhancement for gas heat exchangers fitted with porous media", *International Journal of Heat and Mass Transfer*, Vol. 47 No. 23, pp. 4939-4952.

Prasad, V. (1986), "Numerical study of natural convection in a vertical, porous annulus with constant heat flux on the inner wall", *International Journal of Heat and Mass Transfer*, Vol. 29 No. 6, pp. 841-853.

Prasad, V. and Chui, A. (1989), "Natural convection in a cylindrical porous enclosure with internal heat generation", *ASME Journal of Heat Transfer*, Vol. 111 No. 4, pp. 916-925.

Prasad, V. and Kulacki, F.A. (1985), "Natural convection in porous media bounded by short concentric vertical cylinders", *Journal of Heat Transfer*, Vol. 107 No. 1, pp. 147-154.

Rao, Y. and Wang, B.X. (1991), "Natural-convection in vertical porous enclosures with internal heat-generation", *International Journal of Heat and Mass Transfer*, Vol. 34 No. 1, pp. 247-252.

Reddy, B.V.K. and Narasimhan, A. (2010), "Heat generation effects in natural convection inside a porous annulus", *International Communication in Heat and Mass Transfer*, Vol. 37 No. 6, pp. 607-610.

Reddy, P.V. and Narasimham, G.S.V.L. (2008), "Natural convection in a vertical annulus driven by a central heat generating rod", *International Journal of Heat and Mass Transfer*, Vol. 51 No. 19, pp. 5024-5032.

Rong, F., Guo, Z., Chai, Z. and Shi, B. (2010), "Lattice boltzmann model for axisymmetric thermal flows through porous media", *International Journal of Heat and Mass Transfer*, Vol. 53 No. 23, pp. 5519-5527.

Roschina, N.A., Uvarov, A.V. and Osipov, A.I. (2005), "Natural convection in an annulus between coaxial horizontal cylinders with internal heat generation", *International Journal of Heat and Mass Transfer*, Vol. 48 No. 21, pp. 4518-4525.

Rudraiah, N., Shrimani, P.K. and Friedrich, R. (1982), "Finite amplitude convection in a two component fluid saturated porous layer", *International Journal of Heat and Mass Transfer*, Vol. 25 No. 5, pp. 715-722.

Shi, K.F. and Lu, W.Q. (2005), "Numerical simulation of double-diffusive convection with cross gradients", *Journal of Engineering Thermophysics*, Vol. 26 No. 2, pp. 328-330.

Shi, K.F. and Lu, W.Q. (2006), "Time evolution of double-diffusive convection in a vertical cylinder with radial temperature and axial solutal gradients", *International Journal of Heat and Mass Transfer*, Vol. 49 No. 6, pp. 995-1003.

Sung, H.J., Cho, W.K. and Hyun, J.M. (1993), "Double-diffusive convection in a rotating annulus with horizontal temperature and vertical solutal gradients", *International Journal of Heat and Mass Transfer*, Vol. 36 No. 15, pp. 3773-3782.

Tan, Z. and Howell, J.R. (1989), "Combined radiation and natural convection in a participating medium between horizontal concentric cylinders", *Heat Transfer Phenomena in Radiation, Combustion and Fires*, Vol. 106, pp. 87-94.

Teamah, M.A. and Shoukri, M. (1995), "The effect of aspect and curvature ratios on double-diffusive natural convection in a vertical annulus", *Alexandria Engineering Journal*, Vol. 34 No. 2, pp. 95-105.

Teamah, M.A., Sorour, M.M. and Saleh, R.A. (2005), "Mixed convection between two horizontal concentric cylinders when the cooled outer cylinder is rotating", *Alexandria Engineering Journal*, Vol. 44, pp. 347-360.

Trevisan, O.V. and Bejan, A. (1986), "Mass and heat transfer by natural convection in a vertical slot filled with porous medium", *International Journal of Heat and Mass Transfer*, Vol. 29 No. 3, pp. 403-415.

Vadasz, P. (2008), *Emerging Topics in Heat and Mass Transfer in Porous Media*, Springer, New York, NY.

Vafai, K. (2005), *Handbook of Porous Media*, 2nd ed., Taylor & Francis, New York, NY.

Yang, Y.T. and Hwang, M.L. (2009), "Numerical simulation of turbulent fluid flow and heat transfer characteristics in heat exchangers fitted with porous media", *International Journal of Heat and Mass Transfer*, Vol. 52 No. 13, pp. 2956-2965.

Yoo, J.S. (1998a), "Mixed convection of air between two horizontal concentric cylinders with a cooler rotating outer cylinder", *International Journal of Heat and Mass Transfer*, Vol. 41 No. 2, pp. 293-302.

Yoo, J.S. (1998b), "Natural convection in a narrow horizontal cylindrical annulus: Pr $<$ 0.3", *International Journal of Heat and Mass Transfer*, Vol. 41 No. 20, pp. 3055-3073.

Yoo, J.S. (1999a), "Prandtl number effect on bifurcation and dual solution in natural convection in a horizontal annulus", *International Journal of Heat and Mass Transfer*, Vol. 42 No. 17, pp. 3279-3290.

Yoo, J.S. (1999b), "Transition and multiplicity of flows in natural convection in a narrow horizontal cylindrical annulus: Pr = 0.4", *International Journal of Heat and Mass Transfer*, Vol. 42 No. 4, pp. 709-722.

Corresponding author
Mourad Moderres can be contacted at: mouradw002@gmail.com